

Microwave Dynamics of Josephson Structures with Nontrivial Current–Phase Relation

G. A. Ovsyannikov, K. Y. Constantinian, Yu. V. Kislinskii, P. V. Komissinskii,
I. V. Borisenko, T. Yu. Karminskaya, and V. K. Kornev

Received March 29, 2006

Abstract—The electrophysical and dynamic parameters (Shapiro steps and detector response) of hybrid heterostructures based on oxide superconductors with the *d*-wave symmetry of the order parameter are studied. Deviation of the current–phase relation from the trivial (sinusoidal) form is revealed. It is shown in terms of a generalized Resistive Shunted Function model with the junction capacitance and higher harmonics of the current–phase relation has virtually no influence on the width of harmonic Shapiro steps but changes the scale of the step-width dependence on the ac current of an external electromagnetic field. In addition, it is shown that these dependences have no local minima if the current–phase relation (CPR) contains harmonics higher than the first. For heterostructures, the amplitudes and signs of the CPR harmonics are determined through comparison of theoretical and experimental data.

PACS numbers: 74.81.Fa

DOI: 10.1134/S1064226906090087

INTRODUCTION

Progress toward creating a quantum computer—a new direction in quantum superconducting electronics—is currently related to the 2ϕ -period component in the current–phase relation (CPR) of a superconducting Josephson junction, $I_s(\phi) = I_c \sin \phi + I_{c2} \sin(2\phi)$, where I_c is the critical current (for example, see [1]). The second harmonic of the CPR, $I_{c2} \sin(2\phi)$, has been observed in superconductor/ferromagnetic/superconductor junctions, which are currently regarded as the most promising elements of quantum computers [2]. For superconductors with isotropic *s*-wave symmetry of the order parameter (*S* superconductors), deviation of the CPR from the trivial form $I_s = I_c \sin \phi$ is known in the case of Josephson thin-film bridges [3]. In Josephson structures comprised of oxide superconductors with high critical temperatures (for example, $\text{YBa}_2\text{Cu}_3\text{O}_x$ (YBCO)), the *d*-wave symmetry of the order parameter dominates in the *ab* plane (*D* superconductors) [4, 5]. In such structures, the second harmonic appears in the CPR owing to the specific properties of this type of symmetry as well as to the formation of low-energy Andreev states [6–8]. Experimentally, second harmonic was found in the CPR of *D/D* and *S/D* superconductor structures [9–11]. However, influence of a nontrivial CPR on the dynamics of Josephson junctions at microwave frequencies has not been studied.

In this study, we experimentally investigate microwave parameters of Josephson *S/D* structures with considerable deviations from the trivial relation $I_s = I_c \sin \phi$. On the basis of the generalized Resistive Shunted Function model of a Josephson junction, a procedure is con-

structed to use the experimental dynamic parameters of the junction for determination of the amplitude of the CPR's second harmonic; the theoretical and experimental results are compared. Experimental samples are Nb/Au/YBCO heterostructures fabricated on an tilted film, which allowed electron transport along the [110] direction in the *ab* plane of the YBCO.

1. EXPERIMENTAL PROCEDURE

$\text{YBa}_2\text{Cu}_3\text{O}_x$ films were grown on (7 10 2) NdGaO_3 substrates. The *c* axis of an epitaxial YBCO film grown on this substrate lies in the (110) YBCO plane and is deflected from the normal to the substrate plane by an angle of $\approx 11^\circ$. A detailed X-ray study of the YBCO films revealed that, during the film growth, the epitaxial relation (001) YBCO || (110) NGO is preserved and the film orientation is close to (1 1 20) YBCO [8]. More detail on the Nb/Au/YBCO fabrication technology can be found in [8, 10]. After the final formation by photolithography, the heterostructures were squares of side $L = 10\text{--}50 \mu\text{m}$.

The *I*–*V* curve of heterostructures were measured under the conditions of a current bias at $T = 4.2 \text{ K}$, including irradiation of heterostructures with monochromatic electromagnetic waves at a frequency ranging from 36 to 79 GHz. In addition, voltage dependences of the selective detector response were measured at frequencies in the range 36–120 GHz. The dependence of the critical current on the field dependence, $I_c(H)$, was measured for fields up to 10 Oe since, above this level, the results become irreproducible,

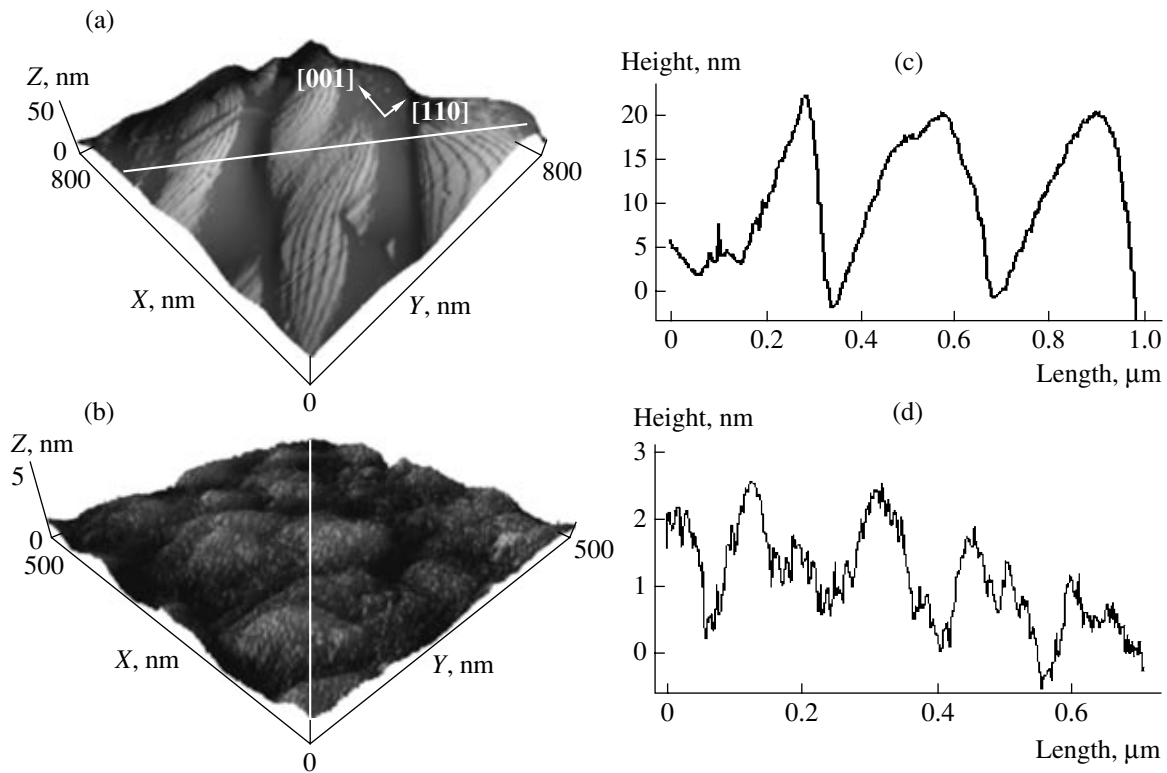


Fig. 1. (a, b) Atomic-force microscopy images and (c, d) profiles of the YBCO films with (a, c) (1 1 2 0)- and (b, d) *c*-orientations. The profiles are taken along the cross-sections through the white lines.

most likely because of the Abrikosov vortices penetrating into the film electrodes.

2. EXPERIMENTAL RESULTS

The surface morphology of as-prepared YBCO films was observed under an atomic-force microscope.

A. Faceting of the (1 1 2 0) YBCO Film Surface

The study of the surface of the YBCO films grown on tilted (7 10 2) NdGaO₃ substrates shows that the film surface consists of relatively large growth steps substantially exceeding inhomogeneities of the substrate surface both in width and height (Figs. 1a, 1c). The height of the growth steps ranges from 15 to 20 nm, and with a change in the facet orientation, the facet length along the substrate surface varies in the range 0.02–0.20 μm. The YBCO surface roughness along the facets does not exceed 2 nm [8]. Note that a *c*-oriented YBCO film deposited on a standard, for example, (001) SrTiO₃ substrate has no clearly defined growth directions (Figs. 1b, 1d). Since the (1 1 2 0) YBCO-film surface consists of facets that are normal to the [001] and [110] YBCO directions, the heterostructure obtained after the Nb sputter deposition consists of an array of contacts to the (001) and (110) crystallographic planes of YBCO.

The *S/D_c*-type junctions are formed on the YBCO (001) facets (Fig. 2a). The critical current of such contacts is proportional to the squared value of barrier transparency \bar{D} owing to the *d*-wave symmetry of the order parameter of the *D* electrode and must depend mainly on the second harmonic of the CPR. In the experiment, critical current of the *S/D_c* junctions is determined by the *s*-wave component of the order parameter [12] in the YBCO, Δ_S :

$$I_{c1}R_N \approx \Delta_S\Delta_{Nb}/(e\Delta_D), \quad (1)$$

$$I_{c2}R_N \approx \bar{D}\Delta_{Nb}/e, \quad (2)$$

where e is the charge of an electron; R_N is the resistance in the normal state; and Δ_S , Δ_D , and Δ_{Nb} are the energy gaps of the *D* superconductor and niobium, respectively.

It is assumed in (1) and (2) that the YBCO order parameter is described by the expression $\Delta(\theta) = \Delta_D \cos 2\theta + \Delta_S$, where θ is the angle between the electron momentum and the [100] direction of YBCO. Taking into account the experimental values of the boundary transparency $\bar{D} \approx 10^{-4}$, we obtain the ratio of the harmonics of the CPR, $q = I_{c2}/I_{c1} \approx \bar{D}\Delta_D/\Delta_S \approx 10^{-3}$, for the typical values $\Delta_{Nb}/e = 1.5$ mV, $\Delta_S/e \approx 1$ mV, and $\Delta_D/e \approx 20$ mV [8]. Owing to thermal fluctuations even at a low

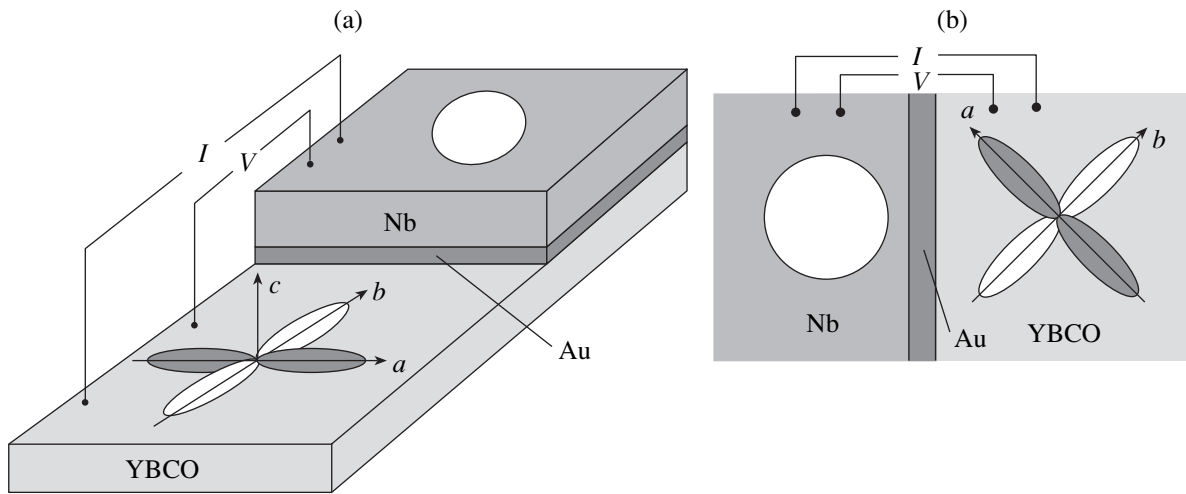


Fig. 2. Schematic diagrams of (a) S/D_c and (b) S/D_{45} junctions. The d -wave and s -wave order parameters are shown schematically.

temperature ($T = 4.2$ K), such deviations of the CPR from the sinusoidal form cannot be detected experimentally. Note that the values of $q \approx 0.1$ measured in [10, 12] probably have causes that were not taken into account in calculations [8].

The contacts between the (110) YBCO film and Nb form S/D_{45} -type superconducting junctions (Fig. 2b). The supercurrent across them is described by relations similar to (1) and (2); however, an additional current channel arises because of the specificity of the Andreev reflection from the interface between the (110) D -superconductor and the normal metal (or S superconductor). As a result, the second harmonic of the CPR for the S/D_{45} junctions increases noticeably up to the value

$q \approx \Delta_D^3 \bar{D} / (k_B T \Delta_S \Delta_{Nb} k_B T) \approx 0.8$, where k_B is the Boltzmann constant [13, 14]. This phenomenon increases the critical current of the structure. Such junctions have stable phases in the range $0 < \varphi_0 < \pi$ (φ contacts in what follows). Thus, owing to the two types of facets, the heterostructures under study can be represented as arrays of parallel 0 and φ nanocontacts.

B. Magnetic-Field Dependences of the Critical Current

For heterostructures with $L = 20 \mu\text{m}$, the experimental dependence of the critical current on the magnetic field, $I_c(H)$, is generally close to the Fraunhofer dependence $|\sin H|/H$, which is observed for a lumped Josephson junction in the case $L \approx 2\lambda_J$, where λ_J is the Josephson penetration depth [15] (Fig. 3, dashed line). The deviation of $I_c(H)$ from $|\sin H|/H$ is small in the region of the central maximum and grows as magnetic field $|H|$ increases ($|H| > 5$ Oe); therefore, the supercurrent distribution must be regarded as quasiuniform.

A closer approximation of the experimental dependences $I_c(H)$, especially in the region of high magnetic

fields ($H \geq 5$ Oe), can be obtained via representation of the heterostructure in the form of an array that consists of two types of parallel nanocontacts with different CPRs. The closest fit of thus calculated values of $I_c(H)$ to the experimental values (Fig. 3, solid line) is achieved for the following parameters: the amplitudes of the critical-current densities of the first and second harmonics of the CPRs at the ratios 3.300 and 0.023 for S/D_c and S/D_{45} junctions, respectively, and the junctions' sizes that vary throughout the heterostructure arbitrarily. It is seen from Fig. 3 that the presence of the second harmonic in the CPR leads to the partition of the period of dependence $I_c(H)$. For small values of I_{c2} ,

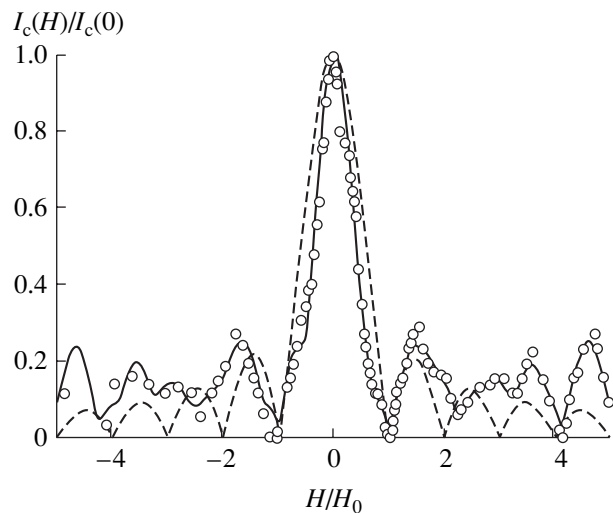


Fig. 3. (Data points) Experimental and (curves) theoretical dependences $I_c(H)$ for the structure with the length $L = 20 \mu\text{m}$. The dashed line is the Fraunhofer dependence, and the solid line is the calculation based on a model with a variable density of the critical supercurrent for a faceted junction [16].

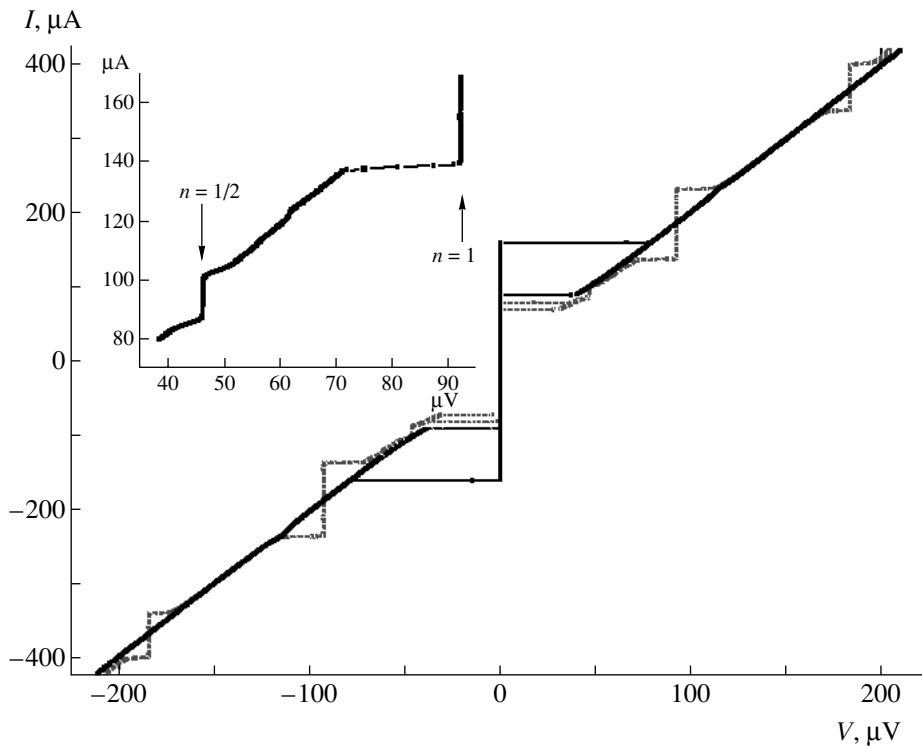


Fig. 4. I - V characteristics for the structures with the length $L = 40 \mu\text{m}$ (solid line) in the absence of an external RF signal and (dashed line) under irradiation at 44.5 GHz. The inset is the I - V characteristic in the vicinity of the subharmonic Shapiro step.

only dips in this dependence are observed. The calculation was performed for 48 facets whose size variations were calculated according to the procedure described in [16].

For the junctions of larger sizes ($L > 30 \mu\text{m}$, dependence $I_c(H)$ differs considerably from $|\sin H|/H$ and its first maximum resembles that in the dependence for distributed junctions, although the condition of a lumped junction $L < 4\lambda_j$ is satisfied. It is shown in [17, 18] that, in the presence of small facets b ($\lambda \ll b \ll \lambda_j$, where $\lambda = 0.15 \mu\text{m}$ is the London penetration depth) strongly varying in the critical current, split Josephson vortices with a fractional part of the magnetic-flux quantum arise. In such structures, the critical current significantly deviates from the Fraunhofer dependence and the period of dependence $I_c(H)$ doubles at $q > 1$. Typical size λ_ϕ of a split Josephson vortex turns out to be substantially less than λ_j , a phenomenon that is likely to be observed in the experiment. Note that λ_j was determined from the critical supercurrent density averaged over heterostructure area A , $\langle j_c \rangle = I_c/A$, with the use of the formula

$$\lambda_j^2 = \frac{\Phi_0}{2\pi\mu_0\lambda\langle j_c \rangle}, \quad (3)$$

where Φ_0 is the quantum of magnetic flux and μ_0 is the permeability of free space.

For $T = 4.2 \text{ K}$ and $\langle j_c \rangle = 1\text{--}10 \text{ A/cm}^2$, the values of λ_j range from 100 to 400 μm , which considerably exceeds the linear size of the junctions under study.

C. Dynamic Parameters of the Structures

Dynamic parameters of Josephson structures are usually determined with the help of Shapiro steps, which appear on the I - V characteristics of junctions placed in an electromagnetic field with frequency f_e [3, 19, 20]. The steps appear owing to the synchronization of the Josephson generation by the external signal. Figure 4 shows the I - V characteristics of the heterostructures without an external action and in the presence of monochromatic field with frequency $f_e = 44 \text{ GHz}$. In addition to the harmonic Shapiro steps observed at $V = khf_e/2e$ (here k is a natural number and h is the Planck's constant), subharmonic steps are seen at $V = (k/l)hf_e/2e$ ($l = 2$). The appearance of subharmonic Shapiro steps in the junctions affected by electromagnetic waves points to the presence of the second harmonic in the CPR [3, 10, 16, 19, 20] (see Fig. 4, inset).

Subharmonic steps were observed for all heterostructures and at all frequencies of the considered external electromagnetic field. However, it is known that subharmonic steps can also be caused by a finite capacitance C of a heterostructure (the McCumber parameter $\beta = 4\pi eI_c R_N^2 C/h > 1$) [20]. The value of β evaluated from the I - V hysteresis was in the range 4–6. In order to dis-

tinguish between the changes that occur in the dynamic properties of the heterostructures owing to the CPR's second harmonic and to the junction capacitance, we performed a detailed study of the microwave-current dependences of critical current, $I_c(I_{RF})$, and of the first Shapiro step width, $I_1(I_{RF})$, and constructed a model for calculating the dynamic parameters of heterostructures with a nontrivial CPR and a finite capacitance $\beta > 1$.

3. ANALYTIC THEORY IN THE HIGH-FREQUENCY LIMIT AND COMPARISON WITH THE EXPERIMENT

In the generalized Resistive Shunted Function model of a Josephson junction with a finite capacitance and the second harmonic in the CPR, the basic equation for the junction under the influence of an external harmonic signal has the form

$$\beta\ddot{\phi} + \dot{\phi} + \sin\phi + q\sin 2\phi = i + I_{RF}\sin(\omega t) + i_f, \quad (4)$$

where $\omega = f_e/f_{c1}$ and $I_{RF} = I_{RF}/I_{c1}$ are the normalized frequency and amplitude of the external signal, respectively; $f_c = 2eI_{c1}R_N/h$ is the typical frequency of the Josephson junction; $i = I/I_{c1}$ is the normalized bias current; and $i_f = I_f/I_{c1}$ is the normalized fluctuation current.

In the limit of the so-called high-frequency approximation, when at least one of the following conditions is satisfied,

$$\omega \gg 1, \quad \beta\omega^2 \gg 1, \quad I_{RF} \gg 1, \quad (5)$$

an analytic solution to Eq. (4) can be obtained in the form of an expansion in terms ranked in decreasing order of smallness. Indeed, in the case under study, term $(\sin\phi + q\sin 2\phi)$ is small in comparison with the other terms in Eq. (4); i.e., it can serve as a small parameter and Eq. (4) can be solved by the method of successive approximations. To this end, the Josephson phase and the constant bias current through the Josephson junction are expanded in a series of corrections with decreasing order of smallness:

$$\phi = \phi_0 + \phi_1 + \phi_2 + \dots, \quad \bar{i} = \bar{i}_0 + \bar{i}_1 + \bar{i}_2 + \dots \quad (6)$$

This expression can be simplified through retention of only the largest term:

$$\begin{aligned} &i_{(2n+1)/2} \\ &= 2\beta \left| J_{n+1}(x)J_n(x)/[(\omega\beta)^2/4 + 1] \right|. \end{aligned} \quad (13)$$

In this case, according to (4), we obtain the set of equations

$$\beta\ddot{\phi}_0 + \dot{\phi}_0 = \bar{i}_0 + I_{RF}\sin(\omega t) + i_f, \quad (7)$$

$$\beta\ddot{\phi}_1 + \dot{\phi}_1 = \bar{i}_1 - \sin(\phi_0) - q\sin(2\phi_0), \quad (8)$$

$$\beta\ddot{\phi}_2 + \dot{\phi}_2 = \bar{i}_2 - \phi_1\cos(\phi_0) - 2q\phi_1\cos(2\phi_0), \quad (9)$$

which yields successive approximations to the solution to Eq. (4). The effect of fluctuations can be analyzed only if they are strong enough ($i_f \gg 1$); for this analysis, fluctuation current i_f in Eq. (7) should be taken into account.

The zeroth approximation obtained from Eq. (7) describes the I - V characteristic of the Josephson junction in the absence of an external field. The first and second approximations obtained from Eqs. (8) and (9) describe either the harmonic and subharmonic Shapiro steps in the case of negligibly small fluctuations ($i_f = 0$) or the harmonic and subharmonic detector responses if the fluctuations are large ($i_f \gg 1$).

A. Shapiro Steps

Sinusoidal CPR ($q = 0$). In this case, Eq. (8) yields the width of harmonic Shapiro steps in the form

$$i_n = 2|J_n(x)|, \quad (10)$$

where

$$x = I_{RF}/\omega \sqrt{(\omega\beta)^2 + 1}. \quad (11)$$

If $\beta = 0$, the above expression coincides with the well-known result for the Resistive Shunted Function (RSJ) model [20]. It is seen that a finite capacitance of the Josephson junction does not change the oscillating character of the Shapiro-step width as a function of external signal I_{RF} but increases the oscillation period.

The next approximation, which can be obtained from Eq. (9), corresponds to the subharmonic Shapiro steps with the width

$$i_{(2n+1)/2} = 2\beta \left| \sum_{m>n} J_{(2n+1)-m}(x)J_m(x)/((\omega\beta)^2((2n+1)/2-m)^2 + 1) \right|. \quad (12)$$

It is seen from (13) that the width of subharmonic step $1/2$ ($n = 0$) is described by the product of the zero- and first-order Bessel functions; for this reason, it oscillates with twice the frequency of the first step as the external signal grows.

Nontrivial CPR ($q \neq 0$). Allowance for the second harmonic in the CPR of a Josephson junction qualita-

tively changes the functional dependence of the harmonic Shapiro step width:

$$i_n = 2 \max_{\Theta} [J_n(x) \sin(\Theta) + q J_{2n}(2x) \sin(2\Theta)], \quad (14)$$

where the maximum of the expression in brackets is taken with respect to phase difference Θ and argument x is determined from (11).

It follows from (14) that second-harmonic normalized amplitude q can be found via analysis of the minima of the experimental critical current and harmonic-step width as functions of i_{RF} . For example, for small q , the critical current attains minimum $I_c(x')$ when $J_0(x') = 0$. The corresponding second-harmonic amplitude can be estimated as $q = I_c(x')/[I_c(0)J_0(2x')]$. For the experimental dependence given in Fig. 5a, this expression yields $q = 0.14$, which is very close to the estimate $q = 0.16$ obtained from the analysis of the minimal width of the first step. For large junctions ($L > 20 \mu\text{m}$), we have higher minimal values of the critical current and first-step width and, therefore, higher values of q . Thus, for $L = 30 \mu\text{m}$, the second-harmonic amplitudes estimated from dependences $I_c(i_{RF})$ and $I_{1/2}(i_{RF})$ (see Fig. 5b) are $q = 0.43$ and 0.34 , respectively. Note that it is impossible to determine the sign of a CPR harmonic through the use of only the dependences of the critical current and harmonic Shapiro step width. To do this, it is necessary to study the dynamics of the formation of fractional Shapiro steps, in particular, the case $k/l = 1/2$.

Expression (14) can be generalized to the case when several harmonics are present in the CPR of a Josephson junction:

$$i_n = 2 \max_{\Theta} \left| \sum_k q_k J_{kn}(kx) \sin(k\Theta) \right|, \quad (15)$$

where k is the harmonic number and q_k is the contribution of the k th harmonic to the supercurrent.

It follows from Eqs. (7) and (8) that the I - V curves of junctions with finite capacitance and the second harmonic in the CPR may show fractional Shapiro steps, in particular, step $1/2$ with the width

$$\begin{aligned} I_{1/2}/I_c = 2 \max_{\Theta} \left\{ \sin(\Theta) \left[q J_1(2x) + \beta \frac{J_1(x) J_0(x)}{(\beta\omega)^2/4 + 1} \right. \right. \\ \left. \left. + 4q^2 \beta \frac{J_2(2x) J_0(2x)}{(\beta\omega)^2 + 1} \cos(\Theta) \right] \right\}. \end{aligned} \quad (16)$$

Comparison of the experimental data with the step width calculated from (16) as a function of the external signal for $q < 0$ and $q > 0$ indicates that, in our case, the second harmonic has a negative sign, $q < 0$. Indeed, the amplitude of the step $1/2$ calculated for $q > 0$, first, substantially exceeds the experimental values and, second,

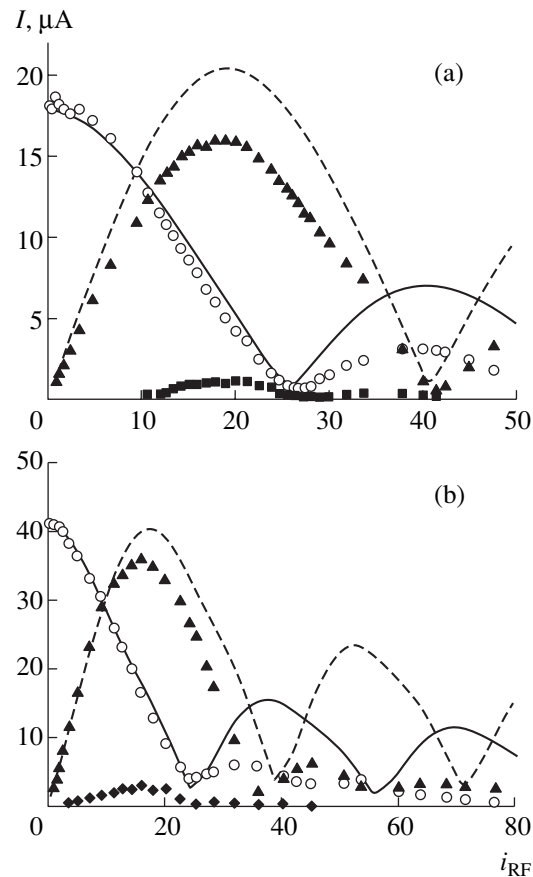


Fig. 5. (Circles and solid line) critical current and the width of (triangles and dashed line) the first and (squares) the fractional (1/2) Shapiro steps vs. normalized microwave current $i_{RF} = I_{RF}/I_{c1}$ for the structures of the lengths $L =$ (a) 20 and (b) 30 μm . Data points represent experimental values; curves, calculated values.

has no local minimum observed experimentally between $i_{RF} = 0$ and the value corresponding to the first minimum of critical current $I_c(i_{RF})$ (Fig. 6). The negative sign of second harmonic q follows from the theoretical calculations carried out for S/D_{45} junctions in [13] and was obtained experimentally for bicrystal Josephson junctions [11].

It is interesting that a small variation of normalized frequency ω of external radiation leads to noticeable change in the dependence $I_{1/2}(i_{RF})$. This result is due to the simultaneous competing effects of the junction capacitance and the nonsinusoidal CPR on the formation of the fractional Shapiro step: the first two terms in (16) corresponding to these factors have opposite signs. On the whole, the experimental behavior of step $1/2$ (Fig. 6) corresponds to theoretical dependence (16), although the maximum value of $I_{1/2}(i_{RF})$ differs several-fold from the theoretical estimate. Note that no adjustable parameters were used in the comparison of the experimental and theoretical results in Fig. 6. The amplitude of the CPR's second harmonic and the scale

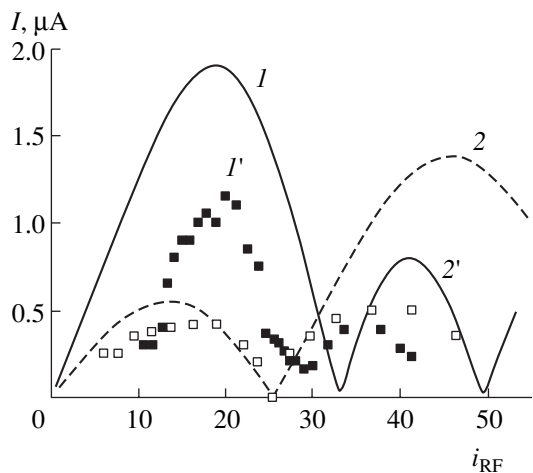


Fig. 6. Width of the subharmonic step vs. normalized microwave current at frequency $\omega = (1$ and $1')$ 1.6 and $(2$ and $2')$ 2.2 for the structures of the length $L = 20 \mu\text{m}$. Data points represent experimental values; curves, calculated values.

of the amplitude of the external electromagnetic field were determined from the comparison of calculated critical current $I_c(i_{RF})$ with the corresponding experimental value (see Fig. 5), while parameter β was calculated from the hysteresis of the autonomous I - V curve [20].

B. Detector Response

Another important dynamic characteristic of the Josephson junction that is strongly affected by a non-trivial CPR and the finite capacitance of the junction is the detector response, η , which reflects a change in the I - V characteristic under the action of a small electromagnetic signal, $\eta = \Delta V(V)$. Much as the second harmonic of CPR gives rise to the fractional Shapiro step, a small external excitation arouses detector response in the vicinity of voltage $V = \frac{1}{2} \frac{hf_e}{2e}$. Figure 7 plots the experimental voltage dependence of the detector response obtained in a wide range of voltages for heterostructures of the size $L = 40 \mu\text{m}$ and with the external-signal frequency $f_e = 77 \text{ GHz}$. It is seen that the amplitude of the subharmonic detector response is several times less than that of the harmonic response. However, the half-width of the Josephson generation line determined from the dependence of the detector response on the voltage applied to the heterostructure (the distance between the maximum and the minimum) was practically the same for both the harmonic and subharmonic responses.

In the case of strong fluctuations, $\gamma \gg 1$, the detector response can be obtained through solution of (7)–(9) via the method of successive approximations for δ -correlated fluctuations of current i_f , i.e., when

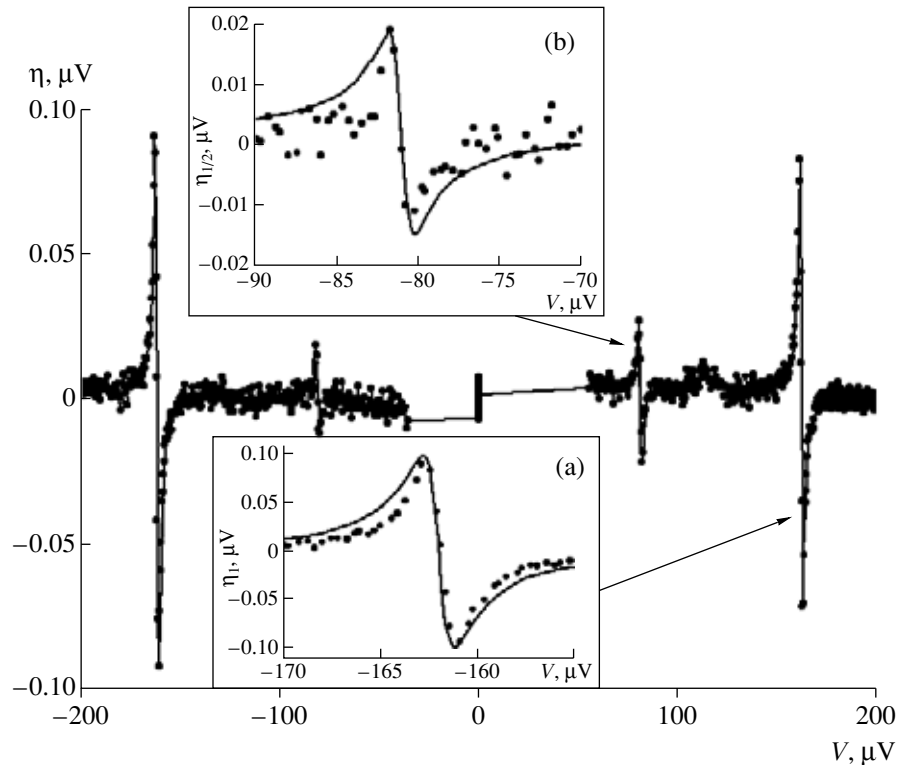


Fig. 7. Detector response of the structures with $L = 40 \mu\text{m}$ to the external signal at 77 GHz. The insets show the (a) harmonic and (b) subharmonic responses to external signal with a lower amplitude. Dots represent experimental values; curves, calculated values.

$\langle i_f(t)i_f(t+\tau) \rangle = 2\delta(\tau)\gamma$ and $\langle i_f(t) \rangle = 0$. Here, γ is the noise factor coinciding with the normalized width of the Josephson generation line. The first approximation contains neither a detector response nor Shapiro steps. The harmonic detector response appears in the second approximation. For small amplitudes i_{RF} of the external signal, the detector response is proportional to i_{RF} raised to the $2n$ th power and, in terms of the standard RSJ model, has the form

$$\eta_n = \frac{1}{2n!^2} \left(\frac{i_{RF}}{2\omega} \right)^{2n} \left[\frac{\delta_n}{\delta_n^2 + \gamma^2} \right], \quad (17)$$

where $\delta_n = v - n\omega$ is the frequency detuning.

Thus, in the region of the first harmonic step ($n = 1$), the detector response has a quadratic dependence on amplitude i_{RF} and decreases drastically with an increase in n . In the generalized Resistive Shunted Function model, which takes into account the capacitance of the Josephson junction and the second harmonic of the CPR, the harmonic detector response for $n = 1$ has the form

$$\eta_1 = \frac{i_{RF}^2}{2\omega^2(\omega^2\beta^2 + 1)} \left[\frac{\delta_1}{\delta_1^2 + \gamma^2} - \frac{\delta_1}{\delta_1^2 + (\gamma + 1/\beta)^2} \right]. \quad (18)$$

The second harmonic of the CPR makes only a small contribution to the harmonic detector response of a Josephson junction and can be derived via consideration of the third approximation. It is seen that the harmonic response decreases with an increase in the capacitance and tends toward zero for $\beta \gg 1$.

In the second approximation of the generalized Resistive Shunted Function model, we additionally obtain a subharmonic detector response in the vicinity of voltage $v = \omega/2$ with its magnitude proportional to the square of CPR's second harmonic amplitude q ,

$$\eta_{1/2} = \frac{q^2 i_{RF}^2}{\omega^2(\omega^2\beta^2 + 1)} \left[\frac{\delta_{1/2}}{\delta_{1/2}^2 + \gamma^2} - \frac{\delta_{1/2}}{\delta_{1/2}^2 + (\gamma + 2/\beta)^2} \right], \quad (19)$$

where $\delta_{1/2} = 2v - \omega$.

It is easily seen that, since $\gamma \gg 1$, the ratio between the harmonic and subharmonic response amplitudes at a fixed power of the external signal is proportional to the squared value of the CPR's second harmonic amplitude:

$$\eta_{1/2}/\eta_1 = 4q^2. \quad (20)$$

Thus, measuring the subharmonic detector response makes it possible not only to confirm the existence of the second harmonic in the CPR of a Josephson junction but also to find this harmonic's amplitude q . The harmonic and subharmonic detector responses calculated from (18) and (19) are in good agreement with the

experimental data obtained in this study, as is shown in the insets to Fig. 7.

CONCLUSIONS

We have conducted an experimental study of the electrophysical and dynamic parameters (Shapiro steps and detector response) of heterostructures based on oxide superconductors having a d -wave order parameter and causing the current-phase relation of the heterostructures to deviate from the trivial form. In larger heterostructures, the amplitude of the second harmonic of the current-phase relation was noticeably higher, which resulted in alteration of the dynamic characteristics of the heterostructures. The dynamic parameters of the Josephson structures were calculated in terms of the generalized Resistive Shunted Function model, which considers the junction capacitance and the second harmonic of the current-phase relation. It is shown that the presence of capacitance in the junction has almost no effect on the Shapiro-step width but changes the scale of the step-width dependence on the current induced by the external electromagnetic field. The presence of harmonics in the current-phase relation leads to the disappearance of local minima in the dependence of the Shapiro-step width on the current induced by the external excitation. This circumstance allows experimental determination of the harmonics' amplitudes, while their sign can be determined through measurement of the subharmonic Shapiro steps. The detector response in the vicinity of the voltage corresponding to the subharmonic step can also be used to determine the contribution of the second harmonic to the current-phase relation.

ACKNOWLEDGMENTS

We are grateful to E. Goldobin and I.I. Solov'yev for useful discussions and valuable comments.

This study was supported in part by the Russian Academy of Sciences under a program of the Physical Sciences Division; the Russian Foundation for Basic Research, project no. 04-02-16818; and the President of the Russian Federation's Foundation for State Support of Leading Scientific Schools and Young Candidates of Sciences, grants NSh-7812.2006.2 and MK-2654.2005.2.

REFERENCES

1. L. B. Ioffe, V. B. Geshkenbein, M. V. Feigel'man, et al., *Nature* **398** (6729), 679 (1999).
2. H. Sellier, C. Baraduc, F. Lefloch, and R. Calemczuk, *Phys. Rev. Lett.* **92** (25), 257005 (2004).
3. V. N. Gubankov, V. P. Koshelets, and G. A. Ovsyannikov, *Zh. Eksp. Teor. Fiz.* **71**, 348 (1976).
4. C. C. Tsuei and J. R. Kirtley, *Rev. Mod. Phys.* **72**, 969 (2000).

5. H. H. Hilgenkamp and J. Mannhart, Rev. Mod. Phys. **74**, 485 (2002).
6. T. Lofwander, V. S. Shumeiko, and G. Wendin, Supercond. Sci. Technol. **14** (5), R53 (2001).
7. L. H. Greene, P. Hentges, H. Aubin, et al., Physica C **387** (1–2), 162 (2003).
8. F. V. Komissinskii, G. A. Ovsyannikov, Yu. V. Kislinskii, et al., Zh. Eksp. Teor. Fiz. **122**, 1247 (2002) [JETP **95**, 1074 (2002)].
9. G. A. Ovsyannikov, I. V. Borisenko, K. I. Konstantynyan, et al., Pis'ma Zh. Tekh. Fiz. **25** (22), 65 (1999).
10. F. V. Komissinskii, G. A. Ovsyannikov, E. Il'ichev, and Z. Ivanov, Pis'ma Zh. Eksp. Teor. Fiz. **73**, 405 (2001) [JETP Lett. **73**, 361 (2001)].
11. E. Il'ichev, M. Grajcar, R. Hlubina, et al., Phys. Rev. Lett. **86**, 5369 (2001).
12. P. V. Komissinski, E. Il'ichev, G. A. Ovsyannikov, et al., Europhys. Lett. **57**, 585 (2002).
13. M. H. S. Amin, A. N. Omelyanchouk, S. N. Rashneev, et al., Physica B **318** (2–3), 162 (2002).
14. R. A. Riedel and P. F. Bagwell, Phys. Rev. B **57**, 6084 (1998).
15. A. Barone and G. Paterno, *Physics and Applications of the Josephson Effect* (Wiley, New York, 1982; Mir, Moscow, 1984).
16. Yu. V. Kislinskii, F. V. Komissinskii, K. I. Konstantynyan, et al., Zh. Eksp. Teor. Fiz. **128**, 575 (2005) [JETP **101**, 494 (2005)].
17. R. G. Mints, Phys. Rev. B **57** (6), R3221 (1998).
18. A. Buzdin and A. E. Koshelev, Phys. Rev. B **67** (22), 220504 (2003).
19. R. Kleiner, A. S. Katz, A. G. Sun, et al., Phys. Rev. Lett. **76**, 2161 (1996).
20. K. K. Likharev and B. T. Ul'rikh, *Systems with Josephson Contacts* (Mosk. Gos. Univ., Moscow, 1978) [in Russian].